A2EI

ACCESS TO ENERGY INSTITUTE

TECHNICAL NOTE

Effect of AC Loads on Solar Generators

ISSUE 02 | FEBRUARY 2026

PREPARED BY:

Frieder Rabl
Senior Engineer
Access to Energy Institute
frieder.rabl@a2ei.org

Johannes Hassel
R&D Engineer
Access to Energy Institute

Table of Contents

Effect of AC Loads on Solar Generators

Abstract

This paper examines the effect of AC loads on solar generators installed by the Access to Energy Institute in Nigeria as backup power supplies. Based on high-resolution load measurements in Nigeria, a portfolio of loads and their characteristic parameters was created. From each load we derived a load test that can be performed in the lab to find out which loads can be supplied by the solar generators and whether this causes damage to the solar generators. These tests show that the loads can cause various direct failures and long-term stress in the power electronics of the solar generators. To reduce these effects we propose changes to the inverter circuitry, and to add hardware extensions in the form of an adapted inrush current limiter (ICL). Subsequent validation tests show that the failure rate dropped from 80% to 20%, while at the same time 20% more loads could be supplied. The findings of this work were used to derive recommendations for the development and installation of backup solar generators, which are expected to extend the service life of the products and thus improve access to an affordable, reliable and sustainable energy supply.

I. Introduction

In recent years, hybrid solar generators have emerged as a valuable solution for energy resilience, combining solar power and grid connectivity to power private households as well as small to medium enterprises (SMEs) with reliable power in regions with weak or inconsistent grid access. Solar generators provide a stable source of AC power during grid outages and eliminate the need for fossil-fuel-based generators.

The focus of the following work is on Nigeria where around 2,000 solar generators were installed and monitored by the A2EI since 2019. This paper examines common loads used in Nigeria and their impact on the power electronics of solar inverters. First, the failures and long-term stress caused by the loads were investigated. Furthermore, inverters and external hardware extensions were adapted to reduce this stress.

II. Good to know - Technical Background of Inverters

Hybrid inverters are central to the operation of solar generators, enabling energy management across different power sources: solar panels, battery storage, and the electrical grid.

These inverters combine several main components:

- **Inverter / Charger:** This bidirectional component enables energy transfer from the grid to the battery (charge mode) or from the battery to the inverter output (inverter mode).
- **PV Charge Controller / MPPT:** Directs the energy from the solar panels to either charge the battery or to provide an additional input to the inverter / charger.
- **Relay / Fuses / Protection:** Essential for safety, these components protect the system from electrical faults.
- **Control Unit / Signal & Control Electronics:** The control unit manages system operations. Signal and control electronics include sensing, communication and control logic to ensure operational efficiency and reliability.

In addition to these core components, a hybrid system also includes PV modules, battery storage and external components such as surge protection devices.

A. Inverter Topologies - Low Frequency

The design of the inverter/charger has a direct impact on system efficiency, robustness, and cost. There are two main types of inverter topologies in hybrid systems:

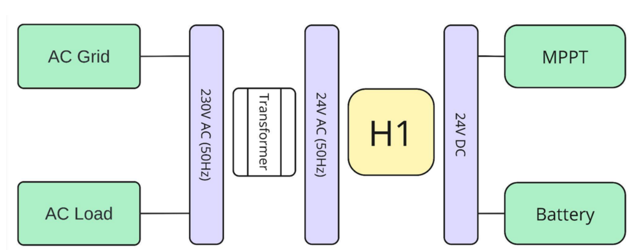

Fig. 1. Low-Frequency Topology with H-Bridge H1

Low-frequency (LF) topologies get their name from the frequency of the central transformer, which converts at 50 Hz line frequency. The power conversion in inverter and charge mode is performed via a DC-AC converter, usually an H-bridge. The H-bridge is also known as a full-bridge converter.

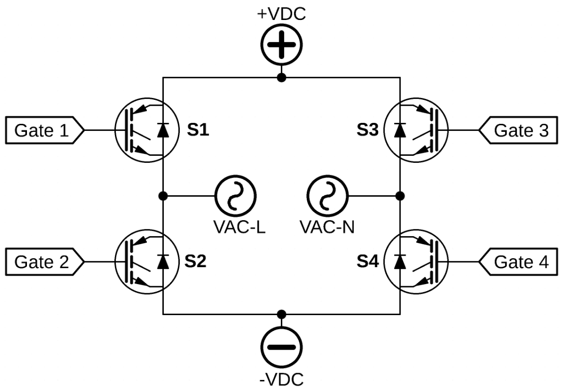

Fig. 2. Simplified H-Bridge

An H-bridge can be divided into two half-bridges. In Fig. 2, S1 and S2 form one half-bridge, while S3 and S4 form the other. A half-bridge consists of a high-side switch (S1 and S3 in Fig. 2) and a low-side switch (S2 and S4 in Fig. 2). A central point for the operation of the H-bridge is that the high-side gate must be switched complementarily to the respective low-side gate, as otherwise a short circuit of the DC side, also known as shoot-through, will occur. A shoot-through leads to permanent damage on the components in the power path. The H-bridge can be used for both inversion and rectification. The switching operations during inversion are relevant when investigating the effect of AC loads and are therefore described shortly after. Some H-bridges have one half-bridge switching in the kilohertz range and one half bridge switching at 50 Hz. Alternatively, both half-bridges can be operated in the kilohertz range. When S1 and S4 are switched on, the positive DC voltage is applied to VAC-L. When S2 and S3 are switched on, the positive DC voltage is applied to VAC-N. In combination with a subsequent low-pass filter and a sine pulse width modulation (PWM) at the gates of the H-bridge switches, a sinusoidal voltage between VAC-L and VAC-N is generated. As semiconductor switches for the H-bridge, metal-oxide semiconductor field-effect transistors (MOSFET) or insulated gate bipolar transistors (IGBT) can be used. Because of their good performance in lower voltage regions, MOSFETs are used for the H-Bridge in LF topologies. Often several MOSFETs are used in parallel to reduce the current flowing through each component. The AC voltage from the H-bridge H1 is then transformed up to mains level via the mentioned LF transformer.

B. Inverter Topologies - High Frequency

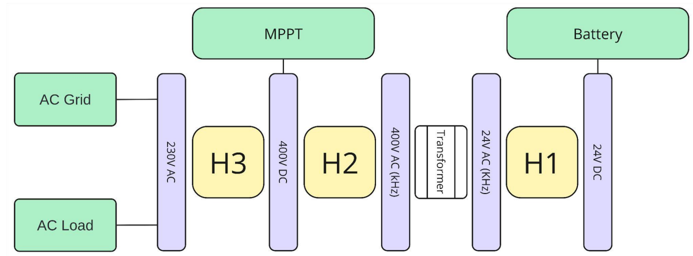

Fig. 3. High-Frequency Topology

High frequency (HF) topologies perform the conversion from low to high voltage at a frequency in the kilohertz range, which allows the use of smaller and lighter transformers. In high-frequency inverters, there are usually 3 conversion stages. First, the battery DC voltage is transformed via a MOSFET H-bridge (H1 in Fig. 3) or a push-pull converter to a high-frequency low AC voltage. From there, the voltage is stepped up to a higher AC voltage level (usually around 400V) with a high-frequency transformer and rectified via another H-bridge (H2) to the DC link circuit. With a final H-bridge (H3), the sinusoidal 230 V output voltage is generated from the DC link voltage. IGBTs are used for H2 and H3 because of their high permissible collector-emitter voltage.
Bidirectional HF topologies use the same path for inversion and rectification. If there are two different power paths for the different modes, the topology is called unidirectional.

III. Understanding Load Realities

The installed solar generators, especially the inverters, showed high failure rates of 20%. Interviews with inverter repair services and distributors have revealed that one of the main causes of failure is the connected load. Hence, 20 typical loads used in households and small businesses with solar backup systems in Abuja, Nigeria, were examined. The field measurements serve as a base for performing tests in the laboratory carried out in Section IV.

A. Collecting Real Data

The focus of this work is on loads that are operated or are intended to be operated using a 230 V AC solar power supply. In order to understand the load-related stress, current and voltage at the load input were measured from start-up until steady state with a 100 MHz oscilloscope. The measurement setup can be seen in Fig. 4.

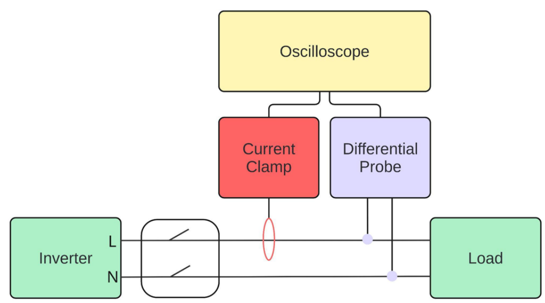

Fig. 4. Load measurement setup

A challenge for the measurements was to maintain comparability while also taking real installation conditions into account. For example, long cables and a high grid impedance dampen the inrush current. In order to keep the measurement realistic, it was decided not to change the installation or cable length during the measurements. A measurement adapter was built to ensure secure and stable contact of the probe heads and is connected between the inverter and the load.

Fig. 5. Measurement adapter

B. Measurement Results

A number of different metrics can be used to compare loads with each other and reproduce them using a programmable load. These characteristics are:

- **Constant load:** Power to operate the load in steady state condition
- **Inrush Current:** Increased current when switching on a load
- **Power Factor:** Phase shift due to inductive or capacitive components
- **Total Harmonic Distortion (THD):** Deviation of current or voltage from a pure sine wave due to harmonic frequencies of higher order
- **Transients:** Sudden nonpower frequency and amplitude change in the steady state condition of voltage or current

TABLE I
Measured loads

Load	Suppli-able with Inverter?	Inrush Currents in A_{peak}	Inrush Duration in s	Transients in A_{peak}	Phase Shift	Constant Load in A_{RMS}
Printer	No	33.6	0.50	—	—	4.2
Sewing Machine 1	Yes	10.4	0.32	—	Inductive	1.4
Sewing Machine 2	Yes	21.6	0.08	—	Inductive	1.6
Drill	Yes	22.4	0.23	—	Inductive	3.3
Bench Grinder	Yes	2.4	12.24	—	Inductive	0.7
Hair Dryer	Yes	—	—	—	—	8.9
Hair Flat Iron	Yes	—	—	—	—	3.5
Hair Drying Hood	Yes	—	—	—	—	1.7
Hair Curling Iron	Yes	—	—	—	—	5.7
Foot Bath	Yes	—	—	—	—	3.0
Freezer	No	21.2	1.03	—	Inductive	1.9
Fridge	Yes	16.4	0.43	—	Inductive	1.8
Gas Oven	Yes	—	—	—	—	0.9
Bread Slicing Machine	No	40.8	0.08	—	Inductive	3.4
Photo Flash	Yes	13.0	1.02	—	Capacitive	0.0
Towel Heater	Yes	—	—	—	—	1.0
Vacuum Cleaner	No	32.8	0.70	—	Inductive	5.4
Air Condition (AC)	No	29.6	0.13	—	Inductive	3.5
Water Pump	No	13.6	0.06	92.0	Inductive	4.5
Microwave	No	—	—	68.0	Inductive	3.7

Some of the 20 loads from Table I can already be powered with existing solar inverters between 500 and 3000 W output power. Other loads can currently not be operated with a solar inverter but with grid supply only as can be seen in Table I.

C. Inrush Current

TABLE II
Loads with high inrush current

Load	Maximum Inrush Current	$I_{max}/I_{constant}$
Bread Slicing Machine	40.8 A	851%
Printer	33.6 A	560%
Vacuum Cleaner	32.8 A	432%
Air Condition	29.6 A	593%
Water Pump	28.0 A	437%

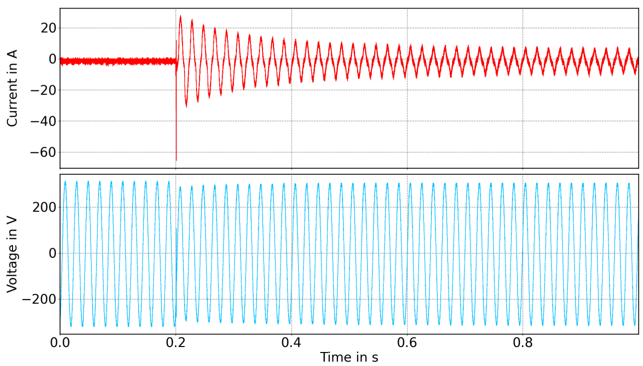

Fig. 6. Inrush current and voltage of a vacuum cleaner

Inrush currents up to 40.8 A_{peak} were measured which is more than eight times the constant load. Hence, loads like the bread slicing machine can not be powered with an inverter with the mentioned power output range, even though their constant current is equiv-alent to other loads that can be used with such an inverter.
In addition to the magnitude of the starting currents, their duration is also an important parameter for the research questions addressed in this technical report. All loads with critical inrush currents reach their steady state after 1.03 seconds or less. The measured magnitude and duration of the inrush current provide important data for the inverter tests and the configuration of an ICL in Section V.

D. Power Factor and THD

Furthermore, the PF and THD of the current can be deter-mined based on the recorded voltage and current.

TABLE III
Loads with smallest non-harmonic power factor and highest THD

Load	Phase Shift	THD of the current	Non-harmonic PF
Bench Grinder	83.3° (inductive)	16.08%	0.12
Bread Slicing Machine	75.0° (inductive)	5.45%	0.26
Microwave	54.7° (inductive)	29.78%	0.55
Photo Flash	76.7°(capacitive)	42.99%	0.21

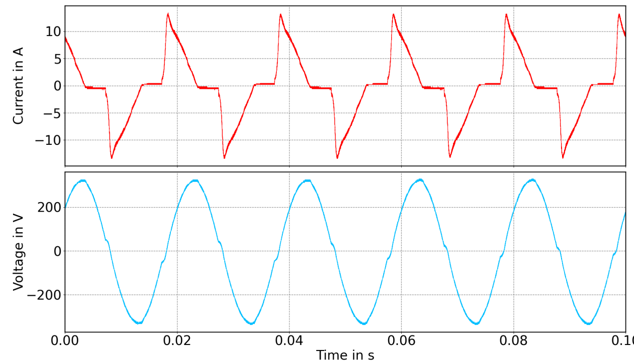

Fig. 7. Current and voltage of a photo flash with capacitive phase shift and THD

The phase shift results from the inductive or capacitive impedance behaviour of the loads. The THD can have various reasons. For example, a non-harmonic load current is generated by the power electronics using phase cutting, as can be seen in Fig. 7. Another reason for the THD can be transients occurring in the microwave's current (see Fig. 8)

E. Transients

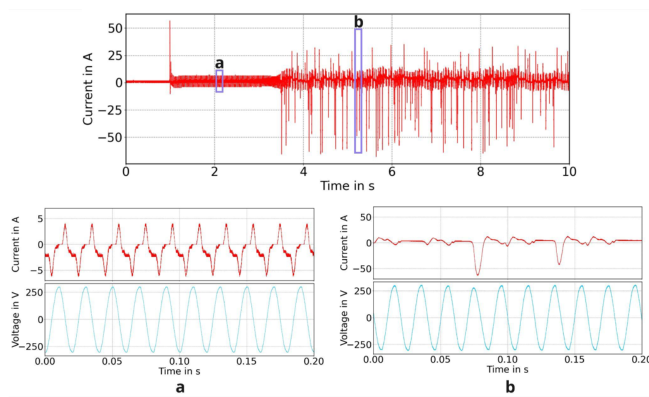

Fig. 8. Current transients and voltage of a microwave

Unexpectedly, two loads showed very high current peaks. These were a microwave and a water pump, both sourced from a second-hand market. In the case of the microwave, these transients sometimes only started after a few seconds as can be seen in Fig. 8. This was accompanied by increased noise.
In some cases, the device also switched itself off after a few seconds. Peak values of 68 A were reached.

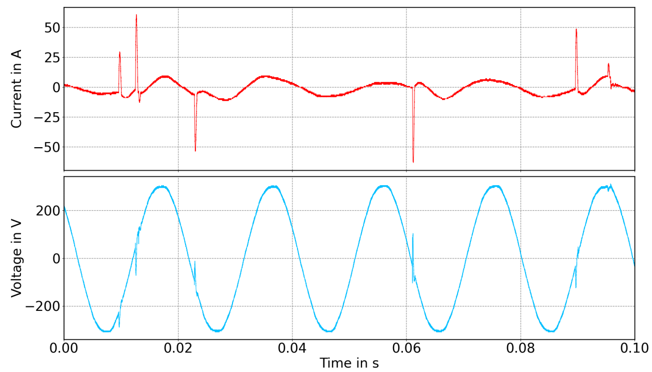

Fig. 9. Current spikes and voltage of a water pump

The water pump was functional but drawing much higher currents than expected according to its rating. A maximum current of 92 A was reached. The pump is based on an electric motor, which can be subject to a winding short circuit if the insulation is damaged. Such a temporary short circuit is a possible explanation for the current peaks measured in the water pump. This can explain why the high currents do occur only in some measurements. The motor was rewound manually which can explain the damaged windings.

F. Measurement Conclusion

Since the early 2000s, international standards such as IEC 61000-3-2 have ensured that CE-qualified loads are subject to THD limits. As a result, many modern loads have power factor correction (PFC) causing a more balanced load on the grid or inverter. As the measurements have shown, the criteria from IEC 61000-3-2 are not met for some of the 20 loads considered. A possible explanation is that PFC was deliberately omitted during the development of the loads in order to reduce costs. In other cases, older devices from the time before those standards were used.

Faulty loads, such as motors with winding faults, are another special case which was examined. Increased loudness, abnormal function or abnormal current waveforms can be an indication of increased power consumption, but often this can only be detected with a high-resolution measurement.

Based on these results, it can be assumed that solar inverters regularly have to supply loads with high starting currents, phase shifts, THD and transients. This puts increased stress on the components of the inverter. In addition, immediate damage can occur in the power electronics, which will be tested in the next chapter.

IV. Inverter Tests

Based on the measurements in the previous chapter, tests were developed for each load scenario to evaluate the effects on the inverters, in the following referred to as device under test (DUT). For this purpose, the recorded loads were simulated using a dynamic AC load to investigate the following three test questions:

1) Can the inverter power the load?
2) Can the inverter power the load with an ICL?
3) Do the loads cause failures or long-term stress on the inverter's power electronics?

TABLE IV
Structure of the inverter tests

Dynamic Load	Test Object	Tested Load Effects	Power Range	Fail Criterion
GW Instek AEL-5000	Inverter only	Inrush Current	80% to 100% rated surge current	DUT can not power load
GW Instek AEL-5000	Inverter only	PF and THD	80% to 100% rated surge current, 0.5 < PF < 1	DUT can not power load
GW Instek AEL-5000	Inverter only	Transients	80% to 100% rated surge current	DUT can not power load
GW Instek AEL-5000	Inverter + ICL	Inrush Current	21 A_{peak} to 40.8 A_{peak}	DUT can not power load
GW Instek AEL-5000	Inverter only	Inrush Current	21 A_{peak} to 40.8 A_{peak}	DUT breaks
GW Instek AEL-5000	Inverter only	PF and THD	22 A_{RMS}, 0.5 < PF < 1, THD up to 50%	DUT breaks
GW Instek AEL-5000	Inverter only	Transients	35 A_{peak} to 75 A_{peak}	DUT breaks
Cinergia EL+20	Inverter only	Load Reproduction	see Table I	DUT can not power load / DUT breaks

For each of these three questions, the inverters were loaded with inrush current, transients and inductive as well as capacitive power factors (see Table IV). A total of five different inverters were tested, which are abbreviated with the following IDs.

TABLE V
IDs of the tested inverters

DUT-ID	Product	Output Power	Topology
BHF1	Hybrid Inverter	2000 W	Bidirectional HF
BHF2	Hybrid Inverter	3000 W	Bidirectional HF
UHF1	Power Station	1200 W	Unidirectional HF
UHF2	Hybrid Inverter	500 W	Unidirectional HF
LF1	Hybrid Inverter	1000 W	LF

A. Test Setup

The dynamic load is connected to the inverter output via a measurement adapter. In the same way as for the load measurements, the inverter output voltage is measured with a differential probe and the output current with a current clamp. With a second 4-channel oscilloscope voltages in the main power path were recorded. The measurement points were selected at the points of common faults. These are the gates of the H-bridges (see Fig. 2) and the DC link bus.

B. Inverters under Stress - What we found

Due to the large number of tests (58 test scenarios per inverter), only test results with particularities are highlighted in the following. Table VI provides an overview of the detected features, long-term stress, and failures.

TABLE VI
Summary of the inverter tests

Feature: (green) Long-term stress: (yellow) Failure: (red)	BHF1	BHF2	UHF1	UHF2	LF1
Internal Current Limitation	Bread Slicing Machine (green)				
Current Spikes			Freezer (yellow)	Water Pump (yellow)	
Output Voltage Overshoot			Micro-wave (yellow)	Water Pump (yellow)	Water Pump (yellow)
Shoot-Through	Vacuum Cleaner (red)			Water Pump (red)	Air Condition (red)
DC Link Anomaly	Vacuum Cleaner (yellow)		Resistive Load (red)		

a) *Internal Current Limitation:*

During a test with inverter BHF1, an unusual switching behavior of the slow-switching IGBT in the AC-side H bridge (H3 in Fig. 3) occurred. The behavior described below appeared during a test with inrush current as can be seen in Fig. 10.

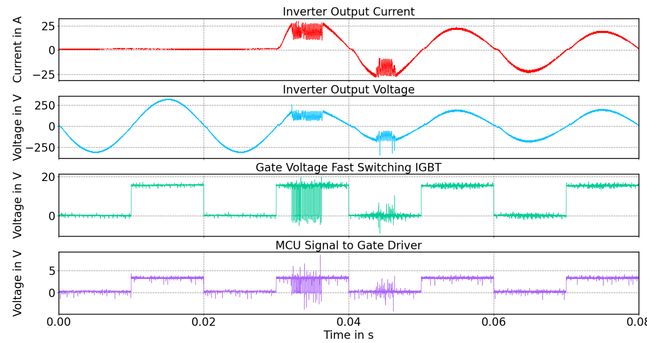

Fig. 10. Internal current limitation of test object BHF1 in response to inrush current

The output voltage shows strong oscillation in the first two half-waves. It can be observed that the low-side IGBT accordingly switches at a frequency of around 6 kHz instead of the normal 50 Hz. This limits the voltage and, as a result, also the current. In order to understand the origin of this switching anomaly, the input signal of the gate driver was measured simultaneously with the gate voltage. Here, this higher-frequency interruption of the 50 Hz PWM also occurs suggesting that this effect is caused intentionally. This switching pattern works as a type of internal current limitation that reduces the duty cycle of the H-bridge and thus protects the power semiconductors from excessive currents. The IGBT is designed for a switching frequency of 70 kHz and is therefore able to withstand this fast switching behavior. Such internal current limiting via the control of the H-bridge is a simple, effective and inexpensive way to limit the current without additional components and extra costs.

b) *Current Spikes:*
When reproducing an inductive load with currents up to 22 A based on the measured freezer, voltage and current ripples with high peaks occurred at the inverter output. The power factor was set to 0.7. This behaviour occurred with the test objects UHF1 and UHF2.

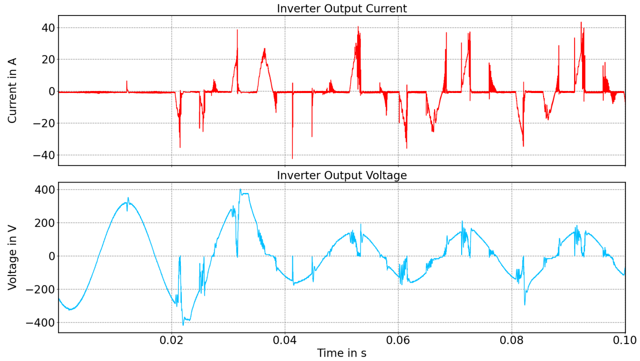

Fig. 11. Current spikes and voltage of test object UHF1 in response to an inductive load

Due to the high load, the output voltage drops, whereupon inverter firmware readjusts the duty cycle of the output-side H-bridge and drives the voltage back up. This control causes output voltage and current ripples that significantly exceed the permissible limits of the inverter's power rating. This results in current spikes up to 50 A with a duration of 20 µs.

Although these currents are still within the rating of the IGBTs used, this high power generates thermal stress, which is the main cause of excessive degradation of the semiconductors and thus results in a shorter lifetime.

The overload protection (OLP) of the DUT is not triggered, even though the maximum permissible peak current is 14.8 A. The threshold time after which the OLP triggers must not be set too low, otherwise switch-on transients will cause a system shut down. However, the settings of DUT UHF1 allow a significant pulse width of high currents, which can occur over several seconds. In contrast to other test objects, the firmware of this inverter does not adequately protect the components.

c) *Output Voltage Overshoot:*

The inverter LF1 shows a significant voltage drop when subjected to transients, followed by an output voltage overshoot of 472 V. The transients were set to 75 A.

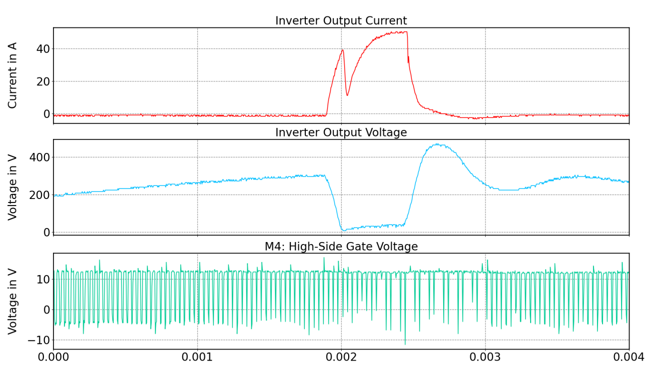

Fig. 12. Output voltage overshoot of test object LF1 in response to current transients

In Fig. 12, it can be seen how the duty cycle is increased to almost 100% when the voltage drops. At t = 0.0025 s, the overvoltage peak is reached. Only at t = 0.003 s, the PWM duty cycle of the AC-side H-bridge (H3 in Fig. 3) is reduced. With this latency of Δt = 500 µs, the control is relatively slow. Comparable inverters such as BHF1 achieve latencies of Δt = 200 µs here.

The large 50 Hz transformer in LF inverters creates a high internal inductance, which causes the voltage to change slowly when the current gradient $\delta I/\delta t$ is large. This means that there is a native latency between the change in the duty cycle of the H-bridge and the resulting voltage change at the inverter output. This makes fast and precise control even more necessary than with HF topologies. We recommend that the control of inverter LF1 has to be upgraded to a maximum latency of Δt = 200 µs.

These overvoltages can damage the loads as well as parts of the power electronics of the inverter. Hence, these overvoltages must be avoided to protect both the solar generator and the customer's appliances.

d) *Shoot-Through:*

Shoot-throughs occur when the gate voltages of the high side and low-side MOSFET/IGBT overlap. The resulting short circuit on the DC side causes thermal destruction of the power semiconductors. Adjacent components, such as gate drivers, are often also affected. Shoot-throughs are one of the most common faults identified in solar generators installed by A2EI and are therefore of particular interest.

1. *UHF2:*

Test object UHF2 was irreparably damaged when subjected to a load of 55 A transients. The test object passed all short duration tests in which the DUT was loaded for a maximum of 30 seconds. As an addition to these tests, an one hour long duration test was performed. The OLP is not triggered here due to the narrow pulse widths of the high currents. After 30 minutes, the system showed a permanent failure.

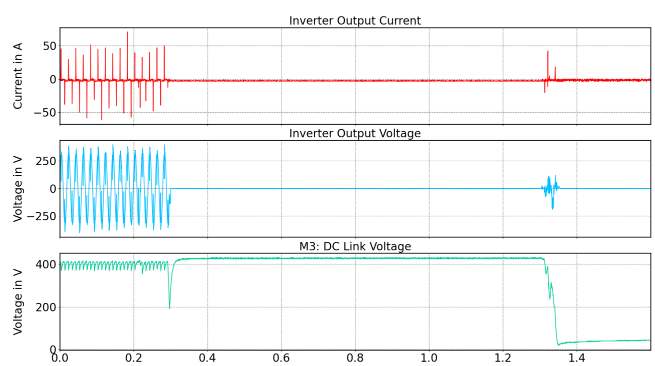

Fig. 13. Shoot-through of test object UHF2 in response to transients

In Fig. 13, it can be seen that at t = 0.3 s that the inverter quickly switches off when the DC link voltage drops. After one second, the inverter tries to start again, completely discharging the DC link within 25 ms. The rapidly dropping voltage of the DC link is a clear indication of a shoot-through in the H-bridge behind it (H3 in Fig. 3).

An analysis of the damaged components confirmed this assumption and revealed that not only the IGBTs of the H bridge but also their drivers had been destroyed. All other components of the H-bridge and the driver circuit were tested individually and found to be functional. After replacing the damaged components, the DC link voltage continued to drop as soon as the fast low-side IGBT was switched on. This indicates a short circuit between the conductor tracks of the corresponding high-side IGBT. Due to this damage to the PCB, the inverter is not repairable.

Shoot-throughs occur when the gate voltages of the high side and low-side MOSFET/IGBT overlap. To avoid this, digital gate drives have a dead time that prevents this overlap of the on state. In the case of the test object UHF2, this dead time at the driver output is 1 µs. However, the actual dead time at the gate of the IGBTs depends on various other parameters. First of all, the current rating of the driver and the gate series resistance determine the edge steepness of the gate signals. A higher gate resistance means slower charging of the gate capacitance and a shorter dead time at the gate. Furthermore, when the IGBTs are switched off, tail current flows, which causes heat dissipation and switching losses. This current can be reduced by applying a negative gate turn-off voltage. The inverter UHF2 uses a TR2113 driver, which does not use a negative turn-off voltage. In addition to the heat generated by the high currents, this further increases the junction temperature of the semiconductor. At a temperature of 120°C, the IGBTs are only rated for 40 A. This current level was exceeded in this test. The temperature increases the turn-off time of the IGBTs, which is why it is assumed that the turn-off time has become so long due to the high thermal stress that the gate signals overlapped resulting

in a shoot-through. This permanent damage can be avoided if the OLP works more precisely.

2. LF1:

Another shoot-through occurred in DUT LF1. In this inverter, the air condition load was reproduced using the dynamic load. For this purpose, inrush current with a 29.6 A_{peak} and an inductive phase shift of 31.3° was set.

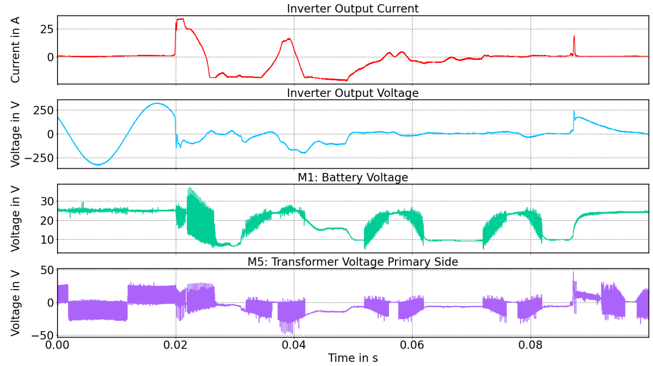

Fig. 14. Shoot-through of test object LF1 in response to inrush current

It can be observed how the battery voltage, which is buffered at the inverter input with several capacitors, drops from 25 V to 6.4 V indicating a high current flow across the H-bridge (H1 in Fig. 1). A subsequent analysis revealed that a total of three MOSFETs and their gate resistors and gate pull-down resistors had failed. The MOSFETs are two high-side and one low-side MOSFET, all located in the same half-bridge. After replacing the components, the inverter is functional again. The transformer voltage in Fig. 14 shows that there is no overvoltage at the semiconductors, which means that the components must have failed due to overcurrent.

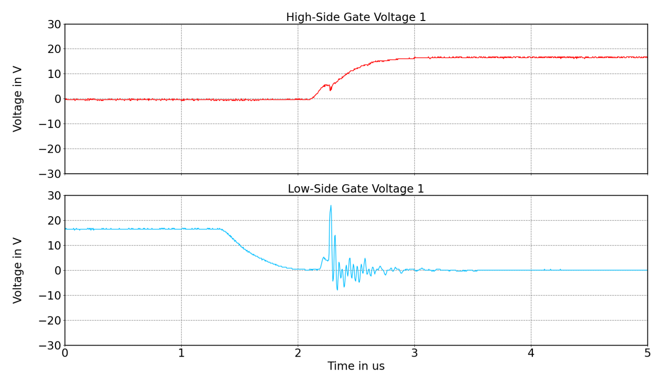

Fig. 15. Crosstalk between high- and low-side gate due to Miller capacity

Crosstalk was detected when the high-side gate was switched on. As can be seen in Fig. 15, switching on the high-side MOSFET causes a voltage glitch at the low-side gate, which leads to a parasitic switch-on. This is caused by the parasitic Miller capacitance of the low-side MOSFET between drain and gate. When the drain-source voltage of the low-side MOSFET rises rapidly due to the high-side MOSFET turning on, a current flows through the Miller capacitance via the gate resistance, which then causes a voltage glitch at the gate. The voltage spike significantly exceeds the threshold voltage, which is the cause of the shoot-through. The gate drive is adapted in Section V.

e) DC Link Anomaly:

1. BHF1:

The reproduction of the vacuum cleaner with the dynamic load resulted in phase jumps, high voltage and current oscillations and an overvoltage in the DC link bus of inverter BHF1. The high currents led to a shoot-through resulting in the destruction of the test object.

The simulated load has a slight inductive phase shift of 9° and a maximum starting current of 32.8 A_{peak}, which decreases continuously over a period of 700 ms. The constant current is 5.37 A_{RMS}.

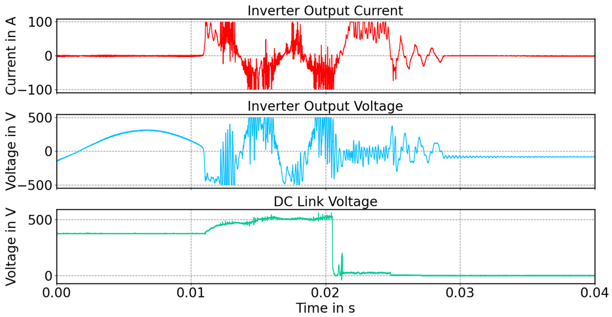

Fig. 16. Output voltage and current phase jumps of test object BHF1 in response to inrush current

The reason of the shoot-through of BHF1 is similar to the one of UHF2, therefore the focus is on the DC link voltage. Although the overvoltage measured here on the DC link circuit does not exceed the permissible V_{CE} of the IGBTs, the 530 V is still significantly higher than the normal 360 V. The DUT has a digital circuit, which measures the DC link voltage and stops charging the DC link circuit in the event of an overvoltage. However, as can be seen here, this circuit appears to be very slow to respond.

2. UHF1:

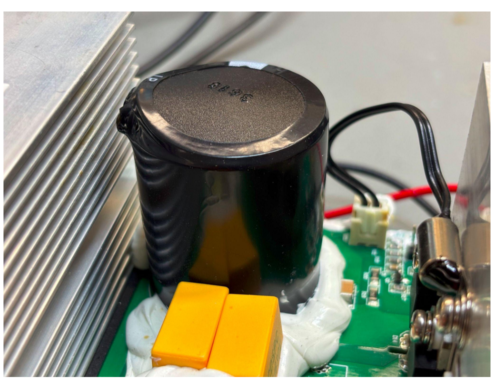

Fig. 17. Blown DC link capacitor of test object UHF1

The DC link capacitor of inverter UHF1 failed. It broke down under load with resistive 860 W after various load tests had already been carried out. No abnormalities in the DC link voltage or switching behavior could be detected, which is why a material defect or fatigue failure of the electrolytic capacitor is assumed. The capacitor was replaced, whereupon tests were carried out with significantly higher loads without any further component failure.

C. Test Conclusion

Overall, 4 out of 5 tested inverters broke down. Two of them even suffered irreparable damage on the circuit board. Furthermore, several effects were observed that do not lead to direct failures but to increased component stress and therefore have a negative impact on the product's lifetime. Table VI gives an overview which simulated load caused what effect for each DUT. The failures correspond to the failures which are observed in the field.

On the one hand, the need to be able to operate loads with higher starting currents, power factor, THD and transients is shown in the load measurements. On the other hand, the results from the inverter tests show that inverters need to be better protected against these loads. The following chapter will discuss whether hardware adjustments can offer both an extension of the usable loads and a protective function.

V. Hardware Adjustments

Two hardware adjustments were made to avoid the failures observed in Section IV.

- First, the gate drive of inverter LF1 will be adjusted to prevent shoot-throughs.
- Second, an adapted ICL will be installed between the inverter and the load to increase the number of loads that can be powered while reducing the load stress on the inverter.

A. Gate Drive

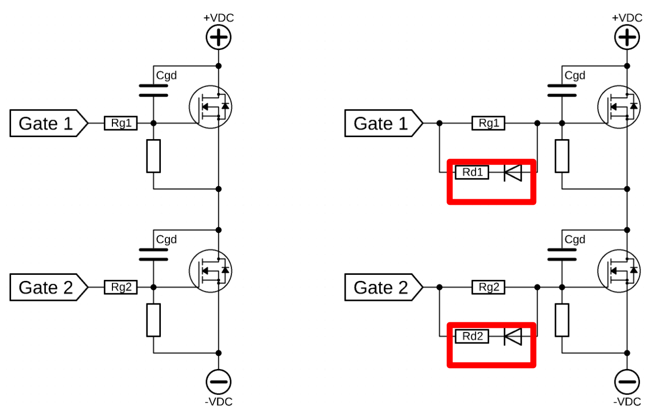

Fig. 18. Original gate drive of test object LF1 and adapted gate drive with fast discharge path

The voltage glitch that occurs at the gate is defined through the Miller current and depends on the following variables.

$$I_{Miller} = C_{gd} \cdot \frac{\delta V_{DS}}{\delta t}$$

$$V_{Gate,Miller} = I_{Miller} \cdot R_g$$

Hence, there are two ways to reduce the Miller effect. Either MOSFETs with lower Miller capacitance C_{gd} are used or the gate drive is adjusted so that the gate is discharged with less resistance R_g. The gate drive is split across two PCBs resulting in long wiring paths with high impedances between the driver and MOSFETs. As Fig. 18 shows, the circuit was adjusted so that a 7.5 Ω resistor R_d with an anti-parallel diode was used in parallel to the 20 Ω gate resistor R_g. The diode must have a low reverse recovery time in order to react quickly to the change in current direction. An SF28 diode with a reverse recovery time of 35 ns was used. This enables faster discharge of the gate and reduces voltage glitches at the gate, as the Miller current can flow via a lower impedance.

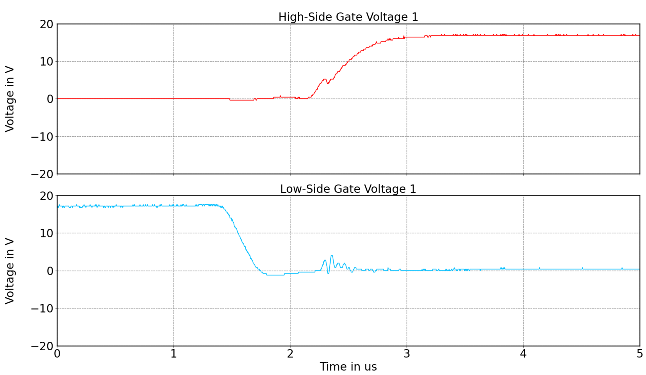

Fig. 19. Reduced Miller effect due to fast discharge path

The adaptation of the gate drive shows a significant reduc-tion of the Miller pulse below the gate voltage threshold voltage of the MOSFET, as can be seen when comparing Fig. 15 and Fig. 19. The faster switching off of the MOSFET can be seen in the higher edge steepness when switching off the low-side MOSFET. The critical tests were repeated with the adapted gate drive.

No more shoot-throughs occurred. Furthermore, in combination with the ICL the hardware adaption now allowed the air condition to be powered by the inverter.

B. Inrush Current Limiter (ICL)

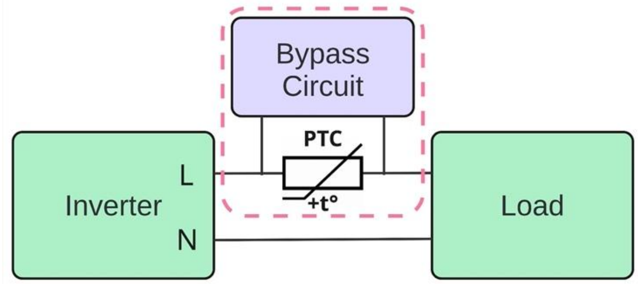

Fig. 20. PTC thermistor with bypass circuit as an ICL

ICLs add impedance to the load path. Here a PTC thermistor is used which increases its resistance at high temperatures. Such a thermistor can only be used with a bypass circuit that bridges the PTC after a certain bypass time. Since ICLs with bypass function are only active for a short period after the load is switched on, they must be located directly in front of the critical loads. They cannot be integrated into the inverter, as the ICL would then already be in bypass mode when critical loads are switched on and would not reliably limit the inrush currents.

Two values are important for limiting inrush currents. First, the impedance determines to what extent the currents are reduced. Second, the bypass circuit sets the bypass time. The ICL was adapted with the aim of attenuating the inrush current of the measured and simulated loads over the full starting time of maximum 1.03 seconds. The attenuation is set so that a maximum current of 19.4 A_{peak} and accordingly a maximum surge power of 3100 W is expected.

Extension of suppliable loads:

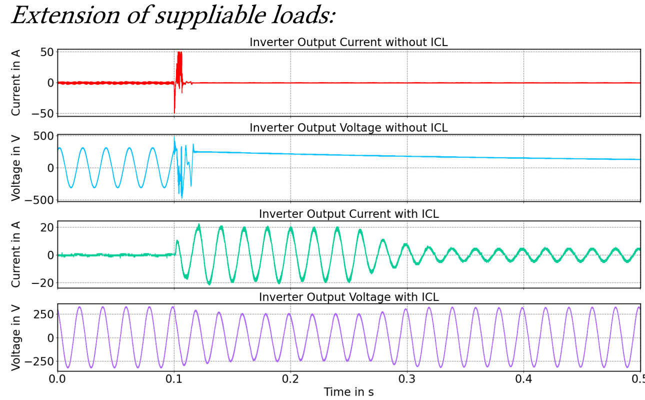

Fig. 21. Output voltage and current of test object BHF1 with and without ICL in response to inrush current

As Fig. 21 shows, the ICL can significantly reduce the inrush current. The currents are attenuated enough to be powered by the inverter. In addition, phase jumps in current and voltage also disappear. As a result, the OLP is no longer triggered and the load can be powered.

b) *Shoot-through prevention:*
The shoot-through from the first iteration of the tests occurred when reproducing the vacuum cleaner on test object BHF1. Without the ICL, this test caused irreparable damage to the inverter. With the ICL connected, the inverter did not show any failure.

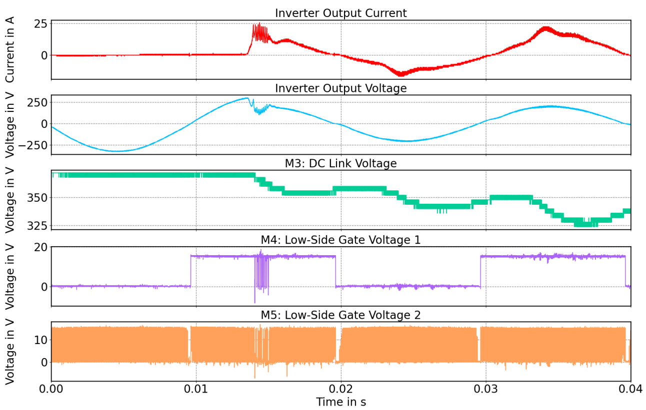

Fig. 22. Output voltage and current of BHF1 with ICL in response to inrush current

As can be seen in the direct comparison of Fig. 16 and Fig. 22, the currents are significantly reduced. The internal inrush current limitation (see Section IV.B.a) can be seen in the slow-switching gate signal M4. The overvoltage in the DC link circuit no longer appears but only shows a slight drop. With the ICL, the OLP is not triggered, which means that the load can be powered. Hence, the ICL can extend the number of suppliable loads and protect the inverter.

c) *DC link capacitor protection:*

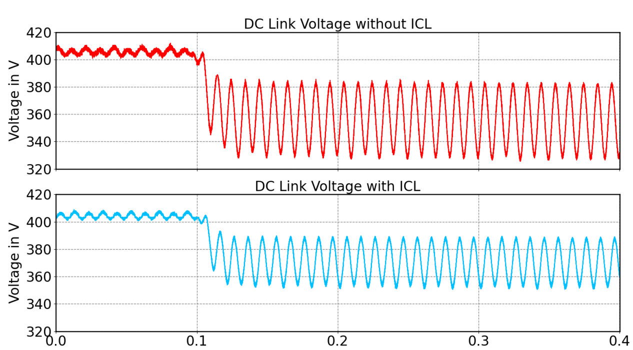

Fig. 23. DC Link Voltage of BHF2 with and without ICL in response to inrush current

The component failure of the DC link capacitor did not occur with the use of the ICL. Fig. 23 shows the DC link capacitor voltage once without and once with the ICL. In both experiments, the inrush current of the bread slicing machine, lasting approximately 80 ms, was reproduced. Comparing the voltage curves, it can be seen that the voltage ripples in the upper plot are slightly larger. At t = 0.1 s, the voltage without ICL drops by 76 V. With the ICL, the voltage drops only by 52 V. The current reduction of the ICL causes this slight smoothing of the capacitor voltage. This reduces the thermal stress on the component. As a result, the risk of fatigue failures is decreased, which has a positive effect on the lifetime of the DC link capacitor. Hence, the ICL has a protective function here.

C. Hardware Adjustments Conclusion

Table VII summarizes how the hardware adjustments offer both an extension of the suppliable loads and a better protection of the inverters.

TABLE VII
Summary of the ICL validation tests

	Without ICL	With ICL
Loads that can be powered	13 of 20 (65%)	17 of 20 (85%)
Inverter failure rate	4 of 5 (80%)	1 of 5 (20%)

As described in Section IV, without the hardware adjustments, 4 of 5 inverters failed during the load tests. With the hardware adjustments, this number was reduced to 1 out of 5. In order to protect test object UHF2 against shoot throughs caused by continuous current transients, both the firmware and hardware of the inverter must be revised. All other DUTs could be protected from damage with simple and low-cost adaptations.
Without the ICL, the inverters BHF1 and BHF2 could only supply 13 of the 20 measured loads. With the ICL, 4 more loads can be supplied.

VI. Recommendations

A. Development Recommendations

The high error rate in the load tests shows that the measured loads have the potential to cause increased degradation and permanent damage in the inverters. Analysis of these errors has resulted in six specific recommendations for the development of solar inverters.

1) The OLP of the inverters must also trigger during current transients. The load tests have shown that the firmware and its protection functions react very differently. Test object BHF2, for example, has a very sharply set OLP.

Inverters UHF1 and UHF2, on the other hand, do not switch off at current peaks that exceed the maximum permissible surge current by more than three times. A compromise must be found here in order to protect the solar generator well on the one hand and not restrict the usable loads too much on the other hand. This compromise could be that transients up to 10 µs only trigger the OLP if they occur more than five times within one second. This prevents the system from being unnecessarily shut down due to switch-on transients and avoids permanent stress from high current transients. The maximum currents must be adjusted to the rating of the MOSFETs/IGBTs. This reduces the failure rate and at the same time does not unnecessarily restrict the number of suppliable loads.

2) The second recommendation to manufacturers addresses the control speed. Some inverters show that control is possible with a latency of 200 µs. Other test objects reacted significantly slower to drops or over shoots in the output voltage. It is recommended to set a latency of maximum 200 µs as a requirement for the output voltage control. This can prevent overvoltages and overcurrents, thereby increasing the lifetime of the inverter.

3) Inverter BHF1 shows a firmware-based current limitation. This works by adjusting the PWM of the output side H-bridge in the event of excessive current so that the voltage is capped. This feature is a cost-effective way to reduce currents while still being able to supply the load.

4) In addition to these three recommendations for a more sophisticated firmware, hardware deficiencies were also discovered. The gate drive of the LF1 inverter exhibited significant crosstalk due to the Miller effect, which leads to parasitic switching of the MOSFETs. To reduce this effect, a fast discharge path must be integrated into the gate drive. This simple and cost effective measure provides better protection for the MOSFETs and reduces the fault rate of the inverters.

5) To better protect the adjacent components of the DC link circuit, an analog DC link overvoltage protection should be integrated. This can quickly and effectively discharge the overvoltages that occurred in various tests.

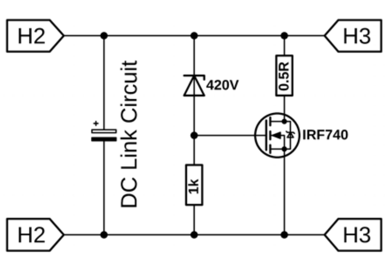

Fig. 24. Active DC link overvoltage protection

A suggested circuit can be found in Fig. 24. The maximum permissible voltage at the DC link circuit is set via the reverse breakdown voltage of the Zener or avalanche diode. If, for example, voltage transients occur due to loads, the Zener diode becomes conductive, switches on the power MOSFET and discharges the voltage against the negative potential of the DC link circuit. This circuit reacts quickly and effectively to overvoltages and protects the components in the H-bridges before and after the DC link circuit.

6) If, after optimizing the OLP, the BHF1 and UHF2 in inverters still suffer from shoot-throughs, the hardware of the IGBT gate drive must be improved. Possible solutions include a faster gate discharge path and the use of negative voltages to switch off the IGBTs.

B. Installation Recommendations

Hardware extensions are an interesting alternative that can be used by distributors and solar installers, to make solar generators more robust. Examples of hardware extensions that are already widely used include surge protection devices and lightning protection devices, which protect solar generators from excessive input voltages. This study confirmed that ICLs are a possible hardware extension for preventing faults caused by overload at the moment of switch-on. They can significantly reduce the failure rate and at the same time, more loads can be powered. ICLs therefore add value for both the customer and the distributor.

1) Distributors are recommended to include ICLs in their product portfolio. It is important to ensure that the current limitation is long enough. The ICL should be active for at least one second and reduce the currents to the maximum permissible surge current of the inverter.

2) Distributors are recommended to analyse the customers loads before installing solar generators. The measurements have shown that the actual load characteristics can differ significantly from their rating and in the worst case damage the inverter. A reliable diagnosis can be made by a high-resolution measurement of the load current. A simple hand-held oscilloscope in combination with a current clamp is sufficient to check if the load poses a threat tothe inverter.

VII. Outlook

This technical note is a result of our "Solar Generator Readiness program" aimed at supporting the energy access sector in improving product quality of solar generators to the benefit of customers while reducing development and warranty costs for manufacturers. By replicating local grid and load conditions and analyzing their impact on solar generators, we hope to contribute to the design of reliable and robust hybrid inverters. Manufacturers and other stakeholders are encouraged to get in touch to collaborate on this matter.At A2EI, we plan to continue publishing technical notes that delve deeper into individual scenarios, exploring specific failure modes and mitigation strategies in greater detail. Additionally, we aim to spotlight challenges that extend beyond grid instabilities and load effects, broadening the scope of this initiative.

We invite the sector to actively contribute by sharing their areas of interest and pressing challenges faced in the field. Collaborative efforts can help shape future investigations and ensure the outcomes are relevant and impactful.

We encourage feedback and input from industry stakeholders on this work. If you have questions, suggestions, or would like to collaborate, please reach out to our team via SolarGenerator@a2ei.org. Together, we can drive meaningful progress.

A2EI

ACCESS TO ENERGY INSTITUTE

OUR WORK IS MADE POSSIBLE BY THE SUPPORT OF OUR FUNDERS:

IKEA Foundation

Stichting DOEN – Nationale Postcode Loterij

Good Energies – Power for a better world

ZE-Gen.

IN COOPERATION WITH:

GGF | results based inventory

THANK-YOU FOR THE SUPPORT:

chromevolt

ACCESS TO ENERGY INSTITUTE

Berlin, Germany | Kampala, Uganda | Abuja, Nigeria

a2ei.org
info@a2ei.org
Access to Energy Institute